J|A|C|S
ARTICLES
Published on Web 04/28/2005

Discovery and High-Throughput Screening of Heteroleptic Iridium Complexes for Photoinduced Hydrogen Production

Jonas I. Goldsmith, William R. Hudson, Michael S. Lowry, Timothy H. Anderson, and Stefan Bernhard*

Contribution from the Department of Chemistry, Princeton University, Princeton, New Jersey 08544

Received December 3, 2004; E-mail: sbernhar@princeton.edu

Abstract: The catalytic process of photoinduced hydrogen generation via the reduction of water has been investigated. The use of parallel synthetic techniques has facilitated the synthesis of a 32 member library of heteroleptic iridium complexes that was screened, using high-throughput photophysical techniques, to identify six potential photosensitizers for use in catalytic photoinduced hydrogen production. A Pd/Ni thin film hydrogen selective sensor allowed for rapid quantification of hydrogen produced via illumination of aqueous systems of the photosensitizer, tris(2,2′-dipyridyl)dichlorocobalt ($[Co(bpy)_3]Cl_2$), and triethanolamine (a sacrificial reductant) with ultra-bright light emitting diodes (LEDs). The use of an 8-well parallel photoreactor expedited the investigation of the hydrogen evolution process and facilitated mechanistic studies. All six compounds investigated produced considerably more hydrogen than commonly utilized photosensitizers and had relative quantum efficiencies of hydrogen production up to 37 times greater than that of $Ru(bpy)_3^{2+}$.

Introduction

The challenge of converting solar radiation into conveniently usable forms of energy is one that has been considered by many researchers. Simple solar devices focus or collect sunlight, harnessing radiation in order to heat dwellings or drive turbines. Photovoltaic cells can convert solar radiation directly to electrical current, but their high cost makes them economically unviable at present. A promising alternative, on which a large amount of research has also been conducted, is the development of catalytic systems that can harness the energy in sunlight and use that energy to split water into hydrogen and oxygen. These systems hold much promise since they allow solar energy to be converted to hydrogen, a fuel with a high gravimetric energy density and clean combustion products. While storage and distribution remain significant factors impeding the implementation of a "hydrogen economy", the greater challenge is to devise a method of hydrogen production that does not depend on the use of nonrenewable resources.

Catalytic systems that have been shown to successfully effect photoinduced hydrogen production[1−3] typically use transition metal complexes as photosensitizers to harvest solar radiation in conjunction with an electron relay which quenches the excited photosensitizer through electron transfer, creating a reactive species which will then reduce protons to diatomic hydrogen gas. Examples of such systems include those based on the photosensitizer $Ru(bpy)_3^{2+}$, the electron relay methyl viologen, and a platinum catalyst.[4−7] Others have been successful employing $Rh(bpy)_3^{2+}$,[8−10] $Co(bpy)_3^{2+}$,[11−14] or other cobalt complexes[15] in place of the methyl viologen. Systems with a variety of other photosensitizers have also demonstrated the photoproduction of hydrogen.[16−18] These systems are extremely complex, often including a dispersed metal catalyst as well as a sacrificial reductant in cases where the reduction of water to hydrogen takes place without the concurrent oxidation to form oxygen. Despite its promising origins in the late 1970s and early 1980s, this field has been somewhat dormant in the past two decades. Due to significant advances throughout the past 20 years, both in analytical techniques and methodology as well as in transition

(1) Darwent, J. R. In *Photogeneration of Hydrogen*; Harriman, A., West, M. A., Eds.; Academic Press: London, 1982; pp 23−38.
(2) Kiwi, J.; Borgarello, E.; Pelizzatti, E.; Visca, M.; Gratzel, M. In *Photogeneration of Hydrogen*; Harriman, A., West, M. A., Eds.; Academic Press: London, 1982; pp 119−146.
(3) Amouyal, E. In *Homogeneous Photocatalysis*; Chanon, M., Ed.; John Wiley & Sons: Chichester, U.K., 1997; pp 263−308.
(4) Kalyanasundaram, K.; Kiwi, J.; Gratzel, M. *Helv. Chim. Acta* **1978**, *61*, 2720−2730.
(5) Moradpour, A.; Amouyal, E.; Keller, P.; Kagan, H. *Nouv. J. Chim.* **1978**, *2*, 547−549.
(6) Kiwi, J.; Gratzel, M. *Nature* **1979**, *281*, 657−658.
(7) Johansen, O.; Launikonis, A.; Loder, J. W.; Mau, A. W. H.; Sasse, W. H. F.; Swift, J. D.; Wells, D. *Aust. J. Chem.* **1981**, *34*, 981−991.
(8) Lehn, J. M.; Sauvage, J. P. *Nouv. J. Chim.* **1977**, *1*, 449−451.
(9) Kirch, M.; Lehn, J. M.; Sauvage, J. P. *Helv. Chim. Acta* **1979**, *62*, 1345−1384.
(10) Chan, S.-F.; Chou, M.; Creutz, C.; Matsubara, T.; Sutin, N. *J. Am. Chem. Soc.* **1981**, *103*, 369−379.
(11) Brown, G. M.; Brunschwig, B. S.; Creutz, C.; Endicott, J. F.; Sutin, N. *J. Am. Chem. Soc.* **1979**, *101*, 1298−1300.
(12) Krishnan, C. V.; Sutin, N. *J. Am. Chem. Soc.* **1981**, *103*, 2141−2142.
(13) Ziessel, R.; Hawecker, J.; Lehn, J. M. *Helv. Chim. Acta* **1986**, *69*, 1065−1084.
(14) Krishnan, C. V.; Brunschwig, B. S.; Creutz, C.; Sutin, N. *J. Am. Chem. Soc.* **1985**, *107*, 2005−2015.
(15) Hawecker, J.; Lehn, J. M.; Ziessel, R. *Nouv. J. Chim.* **1983**, *7*, 271−277.
(16) Krasna, A. I. *Photochem. Photobiol.* **1979**, *29*, 267−276.
(17) Johansen, O.; Mau, A. W. H.; Sasse, W. H. F. *Chem. Phys. Lett.* **1983**, *94*, 107−112.
(18) Ballardini, R.; Juris, A.; Varani, G.; Balzani, V. *Nouv. J. Chim.* **1980**, *4*, 563−564.

10.1021/ja0427101 CCC: $30.25

metal chemistry, it seems appropriate to reconsider this area of research.

Since Merrifield's pioneering work[19] in 1986, combinatorial techniques[20−22] have been widely adopted in areas including drug discovery[23] and materials synthesis.[24] These techniques are applicable to complex problems with many degrees of freedom, and we have previously used combinatorial synthesis in concert with high-throughput screening techniques to greatly accelerate the discovery of luminophoric ionic iridium complexes.[25] Not all of the compounds synthesized were suitable for the OLED applications that were being pursued, but we recognized that some of these materials could potentially serve as excellent photosensitizers in homogeneous catalytic photoinduced hydrogen production systems.

Recently, combinatorial techniques have been applied to the study of photoinduced oxygen production via the oxidation of water with colloidal transition metal particles.[26] Here, we report on the successful implementation of combinatorial synthesis and high-throughput parallel screening techniques for the discovery of novel photosensitizers that catalyze photoinduced water reduction to yield hydrogen gas. In addition to identifying promising photosensitizers, the parallel high-throughput analytical techniques utilized have allowed considerable insight into the mechanisms governing the complex process of photoinduced hydrogen production.

For photoinduced hydrogen production, photosensitizers with large molar extinction coefficients (to efficiently collect radiant energy) and relatively long excited-state lifetimes (to allow electron-transfer quenching to occur) would be desirable. Using the combinatorial techniques that we have applied to OLED discovery,[25] a library of 32 heteroleptic iridium complexes, each with two cyclometalating ligands and one diimine ligand, was synthesized. The photophysical parameters (excited-state lifetime, emission maximum, molar absorptivity, and quantum efficiency) were measured and used to guide the traditional synthesis of a six-compound sublibrary. Each compound in this sublibrary was then used as a photosensitizer in a standard photoinduced hydrogen production scheme. We utilized a hydrogen selective Ni/Pd thin film hydrogen detector to quantify hydrogen production in each system, allowing simple, reproducible, high-throughput measurements to be performed. We demonstrated that all six of the iridium complexes investigated were more effective photosensitizers than the ruthenium complexes typically used.

Experimental Section

Synthesis. Ligands were purchased from Aldrich or synthesized as described previously.[25] The synthesis and characterization of the previously unreported ligands, 5-methyl-2-(2,4-difluoro)phenylpyridine (F_2-mppy) and 5-methyl-2-(2,4-dichloro)phenylpyridine (Cl_2-mppy), are described in the Supporting Information. Solvents and other reagents were purchased from Aldrich and used without further purification. $[Co(bpy)_3]Cl_2$ was synthesized by heating 2,2′-dipyridyl (2.0 g, 12.8 mmol) and cobaltous chloride hexahydrate (0.95 g, 4.0 mmol) at reflux for 12 h in 50 mL of absolute ethanol. The mixture was cooled and added to 300 mL of diethyl ether. The resulting precipitate was collected by filtration and dried in vacuo to yield 1.9 g $[Co(bpy)_3]Cl_2$ (79% yield). Combinatorial synthesis of iridium complexes was carried out as described previously,[25] and the emission, excited-state lifetime, and absorption measurements were performed exactly according to the protocol described in detail.[25] Lifetimes were measured by exciting at 337 nm with an N_2 laser (Laser Science, Inc. VSL-337LRF, 10 ns pulse), and the emission quantum yield (Φ_{em}) for each sample was calculated according to $\Phi_s = \Phi_r(I_s/I_r)(A_r/A_s)$, where the reference complex ($\Phi_r = 6.22\%$) was $[Ir(ppy)_2(bpy)]Cl$ for the parallel synthesis products and the analogous PF_6^- salt for the control products. To utilize these iridium complexes in photoinduced hydrogen production systems, as well as to validate our parallel synthetic methodology, it was necessary to synthesize large (ca. 50 mg) quantities by traditional methods, as described in our previous work.[25] The identity of each compound was confirmed by ^1H and ^{13}C NMR (Varian Inova-500 spectrometer) and electrospray ionization mass spectrometry (Hewlett-Packard 5898B MS Engine). All spectral information can be found in the Supporting Information.

Hydrogen Evolution. Samples for photoinduced hydrogen production were prepared in 40 mL screw-cap glass vials (VWR) with silicone/PTFE septa. Each sample was made up to a volume of 20 mL in 1:1 water:acetonitrile. Samples typically contained 1−6 μmol of the photosensitizer, 50 μmol of $[Co(bpy)_3]Cl_2$ (the electron relay), 5.4 mmol (230 mg) of LiCl, and 11.3 mmol (1.5 mL) of triethanolamine (TEOA) (the sacrificial reductant); 0.4 mL of 37% HCl was added to each solution to adjust the pH downward. Sample vials were capped and deoxygenated by bubbling nitrogen through them for 15 min. Then the samples were degassed under vacuum, through the septum on the vial, at ambient temperature for 15 min to remove all of the dissolved nitrogen. All hydrogen production was carried out with the vials still under vacuum. The vials were then placed in a home-built eight-compartment sample holder and illuminated from below using ultra-bright light emitting diodes (Luxeon V Dental Blue, Future Electronics) (see Figure 1).

These LEDs were chosen because, unlike the xenon lamps typically used in similar experiments, they do not emit any light in the infrared or ultraviolet portions of the spectrum. Additionally, they are modular, allowing for versatility in experimental design, and they are capable of delivering consistently reproducible illumination over extremely long times (lifetime > 50 000 h). These LEDs have a luminous output of 500 mW ± 10% at 465 nm with a 20 nm fwhm and are driven at a 700 mA of current using a Xitanium Driver (Advance Transformer Company). While the output from these LEDs does not cover the entire solar spectrum, the robust, reproducible versatility that is gained from their use is extremely desirable. To allow the screening of photosensitizers that absorb strongly at other wavelengths, future work will incorporate the use of green, red, and white LEDs into our scheme. Each LED is cooled with a Wakefield Engineering 628 heat sink, and the whole apparatus (vials, holder, LEDs) is placed on an orbital shaker (Labline 3540) and shaken and illuminated overnight. After illumination, the sample vials were then backfilled with water in order to bring them to ambient pressure, and 1.0 mL of the bubble of gas trapped in the vial was sampled using a Hamilton SampleLock syringe. This gas sample was injected into a home-built sample chamber in which a hydrogen sensor (H2Scan, RobustHydrogenSensor) was mounted. The sensor was interfaced to a PC, and data were collected using an interface designed in Labview. Prior to each sample injection, the sample chamber was purged with dry nitrogen until the output of the hydrogen sensor returned to its baseline reading (ca. 2 min). Typically, readings were taken 90 s after sample injection to allow the system to equilibrate. Daily calibrations were performed to ensure the accuracy of the sensor.

Quenching and Electrochemical Studies. Samples for quenching studies were prepared in 1:1 water:acetonitrile with the appropriate

(19) Merrifield, B. *Science* **1986**, *232*, 341−347.
(20) Lebl, M. *J. Comb. Chem.* **1999**, *1*, 3−24.
(21) Kassel, D. B. *Chem. Rev.* **2001**, *101*, 255−267.
(22) Balkenhohl, F.; von dem Bussche-Hunnefeld, C.; Lansky, A.; Zechel, C. *Angew. Chem., Int. Ed.* **1996**, *35*, 2288−2337.
(23) Houghten, R. A.; Pinilla, C.; Blondelle, S. E.; Appel, J. R.; Dooley, C. T.; Cuervo, J. H. *Nature* **1991**, *354*, 84−86.
(24) Cawse, J. N. *Acc. Chem. Res.* **2001**, *34*, 213−221.
(25) Lowry, M. S.; Hudson, W. R.; Pascal, R. A., Jr.; Bernhard, S. *J. Am. Chem. Soc.* **2004**, *126*, 14129−14135.
(26) Morris, N. D.; Mallouk, T. E. *J. Am. Chem. Soc.* **2002**, *124*, 11114−11121.

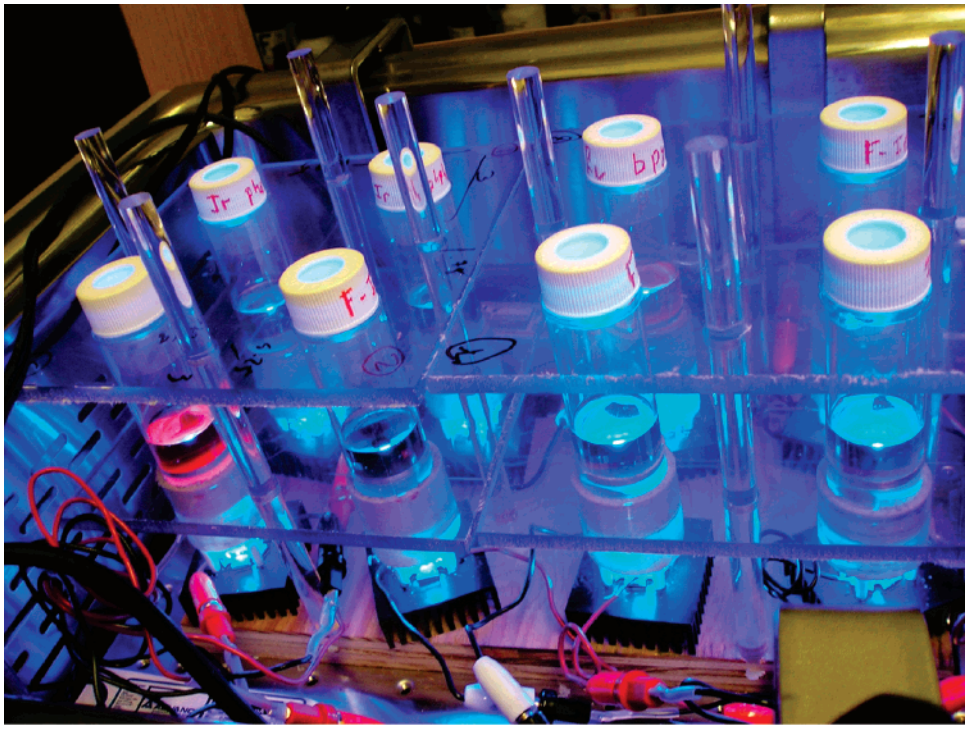

Figure 1. Eight-well photoreactor for parallel photoinduced hydrogen generation experiments.

quencher concentration and a constant photosensitizer concentration of 300 μM. Samples were placed in screw-top quartz cuvettes (Spectrocell) with silicone/TFE septa and degassed with nitrogen for 10 min before measurements were performed. Luminescence lifetimes were measured as described above.

Cyclic voltammetry was carried out using a EG&G PAR 273A potentiostat/galvanostat at a potential sweep rate of 100 mV/s. A homemade platinum disk electrode served as the working electrode, a coiled platinum wire was used as the counter electrode, and a silver wire was used as a pseudo-reference electrode. Electrochemical measurements were carried out in a home-built one-compartment cell at approximately 1 mM photosensitizer concentration in 0.1 M tetra-*n*-butylammonium hexafluorophosphate (TBAH) (Fluka, electrochemical grade) in acetonitrile (Fluka, >99.5% over molecular sieves). Solutions were bubbled with nitrogen for 10 min prior to each measurement to ensure that they were oxygen-free. Ferrocene (Aldrich) was added as an internal standard, and all potentials were subsequently referenced to saturated calomel electrode (SCE).

Results/Discussion

Photophysical Measurements. A library of 32 complexes of the type $[Ir(C\hat{}N)_2(N\hat{}N)]Cl$ was prepared by coordinating two equivalent cyclometalating (C^N) ligands and one neutral ligand (N^N) to an iridium(III) metal center using a parallel synthetic procedure described in our previous work.[25] The 32 products comprise the exhaustive set of combinations of four cyclometalating ligands [C^N = 2-phenylpyridine (ppy), 5-methyl-2-(4-fluoro)phenylpyridine (F-mppy), 5-methyl-2-(2,4-difluoro)phenylpyridine (F_2-mppy), 5-methyl-2-(2,4-dichloro)-phenylpyridine (Cl_2-mppy)] and eight neutral ligands [N^N = 2,2′-dipyridyl (bpy), 4,4′-di-*tert*-butyl-2,2′-dipyridyl (dtbbpy), 4,4′-dimethyl-2,2′-dipyridyl (dmbpy), 4,4′-di-isopropyl-2,2′-dipyridyl (dipbpy), 1,10-phenanthroline (phen), 3,4,7,8-tetramethyl-1,10-phenanthroline (Me_4-phen), 4,4′-diphenyl-2,2′-dipyridyl (dphphen), *cis*-1,2-bis(diphenylphosphino)ethylene (dppe)]. The structure of these ligands can be seen in Figure 2.

The combinatorial products include 20 novel complexes and 12 others that can be appended to an existing library of 100 iridium products previously reported by this group.[25] The novel cyclometalating and neutral ligand combinations were chosen to produce a range of emission maxima, molar absorptivities, and excited-state lifetimes. As seen in Figure 3A, the products of this combinatorial approach display exceptional color versatility ranging from emission in the blue (2.59 eV, 477 nm) to yellow−orange (2.08 eV, 593 nm) regions of the visible spectrum. Similarly, a range of molar extinction coefficients (ϵ, 465 nm) from 384 to 3522 $M^{-1}\cdot cm^{-1}$ was observed (Figure 3B), and the excited-state lifetimes (τ) varied by nearly 2 orders of magnitude from 384 to 13 400 ns (Figure 3C).

Therefore, the combinatorial approach allowed us to obtain a collection of products exhibiting diverse photophysical properties with a relatively modest expenditure of time and resources. To validate this approach and confirm the identity of the combinatorial products, we also synthesized six products by traditional methods; the agreement between the photophysical properties of the traditionally prepared species and the analogous combinatorial products can be seen in Table 1. The six control compounds were selected for use as photosensitizers as discussed below, but in their capacity as controls, they effectively confirm the identity of the combinatorial products and the validity of the measurements. Furthermore, the ability of the combinatorial technique to provide accurate and reproducible results can also be demonstrated by adherence to the energy gap law.[27] As seen in Figure 4A, the agreement between the new library of 32 combinatorial products and the six traditionally prepared species provides convincing evidence that the combinatorial approach is indeed valid. As an indication of the reproducibility of measurements across multiple combinatorial

(27) Kalyanasundaram, K. *Photochemistry of Polypyridine and Porphyrin Complexes*; Academic Press: San Diego, CA, 1992.

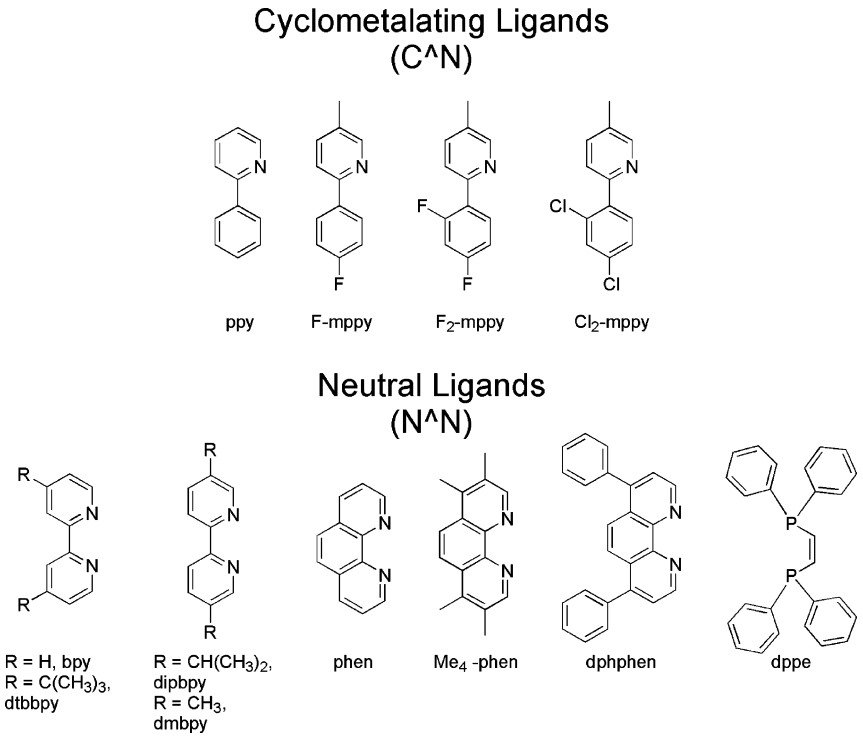

Figure 2. Four cyclometalating (C^N) and eight neutral (N^N) ligands employed in combinatorial synthesis.

attempts, the first library of 100 compounds previously reported[25] is also compared to the new library in Figure 4B. The two data sets demonstrate consistent adherence to the negative slope expected from the energy gap law.

From the combinatorial products, a six-member sublibrary of complexes {$[Ir(C^N)_2(N^N)]PF_6$, where C^N = ppy, F-mppy, and N^N = bpy, phen, dphphen} was traditionally prepared for photoinduced hydrogen production. The six species tested were selected for their absorption and excited-state lifetime properties. Three N^N ligands were chosen primarily because of their tendency to form complexes with large molar extinction coefficients (Figure 3B); presumably, complexes of this type would be desirable for their ability to efficiently capture radiant energy. The choice of C^N ligands, by contrast, reflects the difference in excited-state lifetime among complexes that differ in only their C^N ligand, specifically those containing ppy versus F-mppy. Because the absorption properties remain relatively unchanged upon this substitution, ppy and F-mppy were chosen to examine the effect of a longer lived excited state, exhibited by the latter, on solar energy conversion.

Hydrogen Production. In a typical experiment, hydrogen evolution commenced several minutes after beginning the illumination of the sample. Bubbles (ca. 3−5 mm in diameter) began to rise from within the solution at a vigorous rate, and this continued for 30−60 min. After this time, the bubble production slowed; after overnight illumination, no more bubbles were evident. In some cases, the initially transparent solution became darker when exposed to light. We believe this darkening is due to the generation of a reduced cobalt species as described in the literature,[8] and this will be discussed further below. Analysis of the gas produced typically indicated that it was more than 80% H_2 and in some cases greater than 95% H_2. Since the atmosphere inside our sample vials contains water and acetonitrile vapor, as well as some air due to leakage and imperfect vacuum conditions, the gas produced can reasonably be considered to be effectively composed entirely of hydrogen.

Drawing on previous studies,[3,10,13] the mechanism that we consider to be in effect is as follows:

$$PS + h\nu \rightarrow PS^* \quad (1)$$

$$PS^* + ER \rightarrow PS^+ + ER^- \quad (2)$$

$$ER^- + H^+ \rightarrow ER + 1/2H_2 \quad (3)$$

$$PS^+ + TEOA \rightarrow PS + TEOA^+ \quad (4)$$

where PS is the photosensitizer molecule and ER is the electron relay ($Co(bpy)_3^{2+}$). It should be noted that it takes two cycles through the pathway shown above to generate 1 equiv of hydrogen gas. In certain systems (notably those where an ascorbate buffer is used as the reaction medium), it has been shown that the initial reaction is a reductive (not an oxidative) quenching of the excited photosensitizer by ascorbate.[12,28] By analogy, it might be suspected that TEOA could reductively quench the excited photosensitizer, but Sutin and co-workers showed, for Ru(II)/Co(II)/TEOA systems, that TEOA does not quench the photosensitizer.[13] The ability of TEOA to serve as a two-electron sacrificial reductant has also been postulated,[9] and such a process, where one TEOA molecule can reduce a photosensitizer as well as an electron relay molecule, may be occurring in our system. The only consequence of such a pathway, however, would be the reporting of an inflated turnover number for the $Co(bpy)_3^{2+}$ electron relay.

Table 2 shows the results of photoinduced hydrogen production experiments: the amount of hydrogen produced as well as the number of turnovers that the photosensitizer and electron relay underwent during the course of the experiment. $Ru(bpy)_3^{2+}$

(28) Creutz, C.; Sutin, N.; Brunschwig, B. S. *J. Am. Chem. Soc.* **1979**, *101*, 1297−1298.

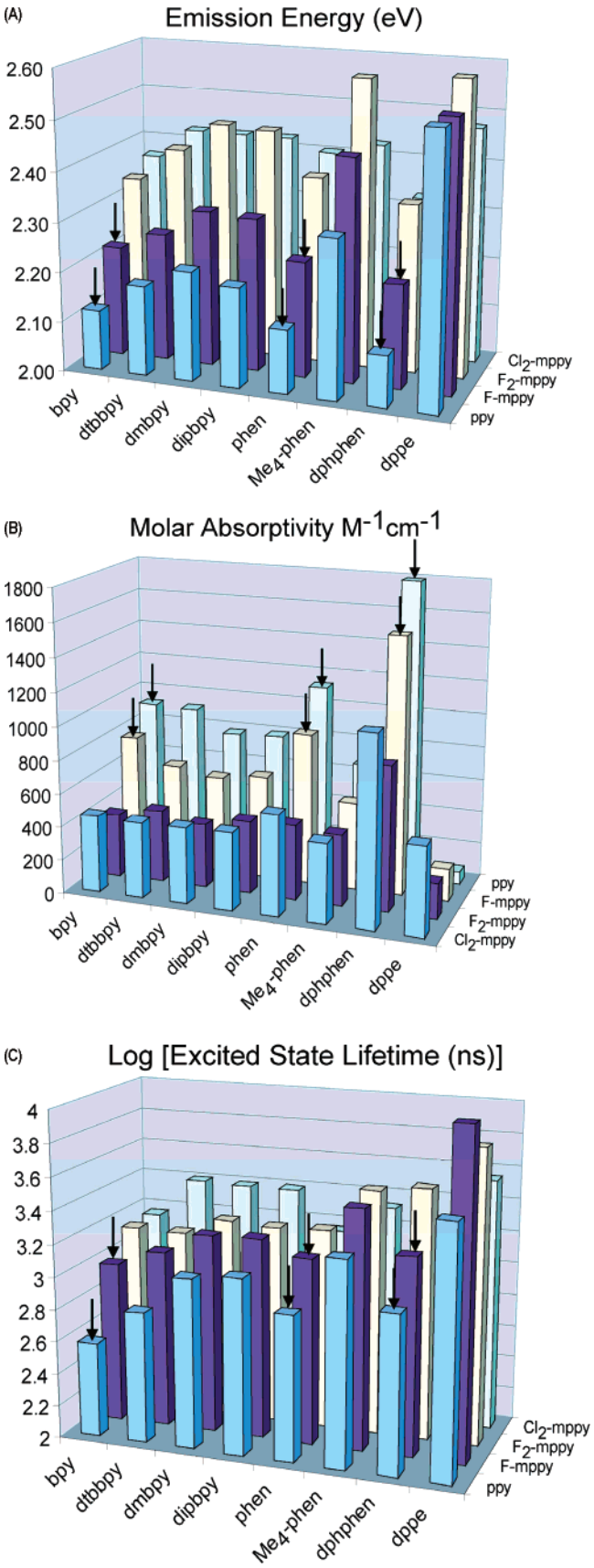

Figure 3. Three-dimensional plots of the emission energy (A), molar absorptivity at 465 nm (the emission maximum of the LEDs) (B), and the log of the excited-state lifetime (C) depict the diversity of photophysical properties exhibited by the combinatorial library. The six compounds chosen for use as photosensitizers in the hydrogen production reaction are designated with arrows.

Table 1. A Comparison of Photophysical Properties between the Six Combinatorial Products and Their Corresponding Controls

sample complex	Cl^{-1}	PF_6^{-1}
$[Ir(ppy)_2(bpy)]^{+1}$	$\Phi = 6.22\%^a$	$\Phi = 6.22\%^a$
$\lambda = 585$ nm	$\tau = 384$ ns	$\tau = 390$ ns
$[Ir(ppy)_2(phen)]^{+1}$	$\Phi = 13.03\%$	$\Phi = 11.86\%$
$\lambda = 579$ nm	$\tau = 786$ ns	$\tau = 783$ ns
$[Ir(ppy)_2(dphphen)]^{+1}$	$\Phi = 10.25\%$	$\Phi = 18.18\%$
$\lambda = 587$ nm	$\tau = 935$ ns	$\tau = 1033$ ns
$[Ir(F\text{-}mppy)_2(bpy)]^{+1}$	$\Phi = 26.85\%$	$\Phi = 21.98\%$
$\lambda = 558$ nm	$\tau = 978$ ns	$\tau = 1049$ ns
$[Ir(F\text{-}mppy)_2(phen)]^{+1}$	$\Phi = 37.10\%$	$\Phi = 33.06\%$
$\lambda = 550$ nm	$\tau = 1397$ ns	$\tau = 1636$ ns
$[Ir(F\text{-}mppy)_2(dphphen)]^{+1}$	$\Phi = 25.17\%$	$\Phi = 32.23\%$
$\lambda = 556$ nm	$\tau = 1645$ ns	$\tau = 1924$ ns

[a] Standard values.

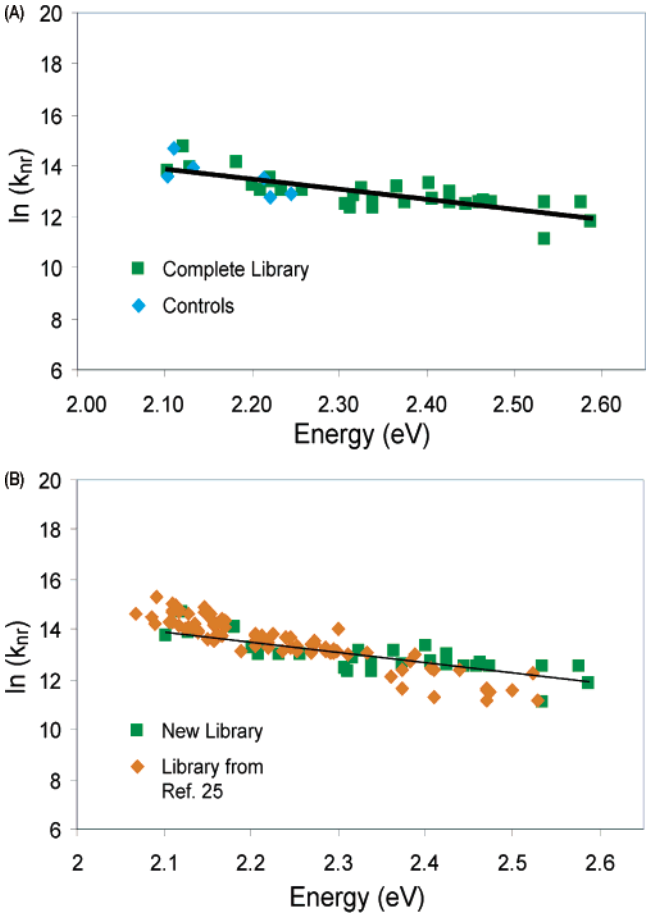

Figure 4. The energy gap law dictates a linear relationship between the natural log of the nonradiative decay rate constant (k_{nr}) and the emission energy. (A) The agreement between the complete library of 32 combinatorial products and the six controls products confirms the validity of the combinatorial technique and the accuracy of the photophysical measurements. (B) The correspondence between the first library previously reported by this group and the new library indicates that the combinatorial technique is accurate and reproducible.

and Ru(4,7-dimethyl-1,10 phenanthroline)$_3^{2+}$ (Ru(dmphen)$_3^{2+}$) are commonly used photosensitizers that have been shown to be among the most effective available.[3] It is clear from our results that all six heteroleptic iridium complexes are considerably more effective than current transition metal based photosensitizer benchmark compounds. While no glaring trends can be determined from the data in Table 2, it does appear that the (F-mppy)-containing compounds, with longer excited-state lifetimes than the corresponding (ppy)-containing compounds,

Table 2. Photoinduced Hydrogen Production[a]

photosensitizer	H_2 evolved (μmol)	PS turnovers	ER turnovers
$Ru(bpy)_3^{2+}$	50	100	2
$Ru(dmphen)_3^{2+}$	290	580	12
$Ir(ppy)_2(bpy)^+$	400	800	16
$Ir(ppy)_2(phen)^+$	430	860	17
$Ir(ppy)_2(dphphen)^+$	420	840	17
$Ir(F\text{-}mppy)_2(bpy)^+$	460	920	18
$Ir(F\text{-}mppy)_2(phen)^+$	430	860	17
$Ir(F\text{-}mppy)_2(dphphen)^+$	430	860	17

[a] All samples have a total volume of 20 mL and contain 50 μM photosensitizer, 2.5 mM $Co(bpy)_3^{2+}$ (electron relay), 0.57 M TEOA, and 0.27 M LiCl in 50:50 water:acetonitrile. The pH was adjusted by the addition of 0.4 mL of 12 M HCl.

produce slightly more hydrogen. It is also important to note that the excited-state lifetimes of all of the iridium complexes studied cover a range similar to that spanned by the two standard ruthenium complexes.[29] It is quite interesting that all of the iridium-based photosensitizers lead to the production of roughly the same amount of hydrogen. This perhaps points to the existence of some process that limits one or more in the series of reactions that leads to hydrogen production.

As a test of our combinatorial methodology, samples from the parallel synthesis described above (chloride salts in ethylene glycol) were also used for photoinduced hydrogen generation by adding the sample in its entirety to the standard H_2O/CH_3CN/TEOA/LiCl/$Co(bpy)_3^{2+}$ reaction mixture. In all cases, hydrogen was produced, but these results cannot be directly compared to those shown in Table 2 due to the presence of the ethylene glycol solvent and differences in photosensitizer concentration. However, the same general trends seen in Table 2 for traditionally synthesized photosensitizers were observed when the parallel-synthesized photosensitizers were utilized for hydrogen production.

The two ruthenium-based photosensitizers mentioned above have much larger molar extinction coefficients than any of the iridium complexes utilized, and in order to more accurately rate the energy harvesting and conversion properties of our iridium complexes, it is necessary to consider this fact. Using the measured extinction coefficients and the photosensitizer concentration, the fraction of incident radiation captured can be determined and used to calculate a relative quantum yield of hydrogen, that is, the amount of hydrogen produced per amount of light energy collected by the photosensitizer. These results can be seen in Figure 5, in which the relative quantum yield of hydrogen for $Ru(bpy)_3^{2+}$ has been set to unity.

This figure demonstrates that these newly synthesized iridium complexes are generally at least 20 times more efficient than $Ru(bpy)_3^{2+}$ and 3−6 times more efficient than $Ru(dmphen)_3^{2+}$ at converting visible light into hydrogen.

Quenching and Electrochemical Studies. To gain a more complete understanding of the complex behavior of these novel photosensitizers, the dynamic quenching of each of the eight photosensitizers utilized, with both $Co(bpy)_3^{2+}$ and TEOA acting as quenchers, was investigated. The luminescence lifetime of each photosensitizer was measured without quencher and in the presence of varying quencher concentrations, and the lifetime ratio (τ_0/τ) was determined and used to calculate k_q, the rate

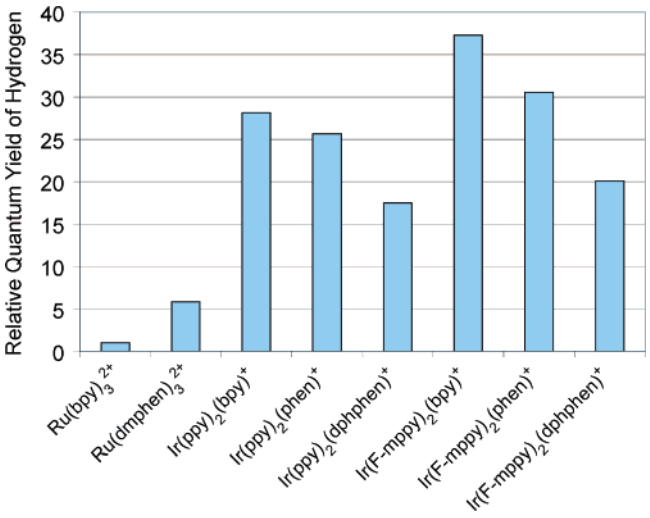

Figure 5. Relative quantum yield of hydrogen for six novel iridium photosensitizers and two standard ruthenium photosensitizers. Relative quantum yield for $Ru(bpy)_3^{2+}$ set to 1.

Table 3. Quenching Kinetics

photosensitizer	k_q $Co(bpy)_3^{2+}$ ($M^{-1}s^{-1}$)	k_q TEOA ($M^{-1}s^{-1}$)
$Ru(bpy)_3^{2+}$	2.3×10^7	no quenching
$Ru(dmphen)_3^{2+}$	1.3×10^8	no quenching
$Ir(ppy)_2(bpy)^+$	4.8×10^8	5.4×10^6
$Ir(ppy)_2(phen)^+$	6.9×10^8	7.7×10^6
$Ir(ppy)_2(dphphen)^+$	6.3×10^8	1.1×10^7
$Ir(F\text{-}mppy)_2(bpy)^+$	4.5×10^8	2.7×10^7
$Ir(F\text{-}mppy)_2(phen)^+$	6.0×10^8	3.4×10^7
$Ir(F\text{-}mppy)_2(dphphen)^+$	4.5×10^8	3.3×10^7

constant for dynamic quenching.[30] As can be seen in Figure 6A−F, all plots of (τ_0/τ) versus concentration are extremely linear ($R^2 > 0.99$ in all cases).

It is notable that neither $Ru(bpy)_3^{2+}$ nor $Ru(dmphen)_3^{2+}$ are quenched at all by TEOA, which is in agreement with the literature.[9,13] The values of k_q for each compound with each of the two quenchers can be seen in Table 3. Somewhat surprisingly, all of the heteroleptic iridium complexes under investigation were quenched by both $Co(bpy)_3^{2+}$ and TEOA, although the rate for quenching by TEOA is approximately 1 order of magnitude slower than the $Co(bpy)_3^{2+}$ quenching rate. It is noteworthy that the iridium photosensitizers are quenched more strongly than their ruthenium-based counterparts by the cobalt electron relay, which correlates with the increased hydrogen production observed.

Electrochemical analyses were performed in order to measure the redox potentials of all eight photosensitizers used, and in conjunction with the spectroscopic data shown in Figure 3A, the excited-state redox potentials were determined.[27] The ground-state redox potentials are shown in Table 4, and the excited-state redox potentials are tabulated in Table 5. $Ru(dmphen)_3^{2+}$ and all six iridium photosensitizers are all considerably more powerful reducing agents than $Ru(bpy)_3^{2+}$, which again is associated with the increased hydrogen production seen with these compounds. The three iridium complexes with F-mppy ligands are all stronger oxidizers than the corresponding iridium ppy complexes, which goes hand in hand with the

(29) Juris, A.; Balzani, V.; Barigelletti, F.; Campagna, S.; Belser, P.; von Zelewsky, A. *Coord. Chem. Rev.* **1988**, *84*, 85−277.

(30) Lakowicz, J. R. *Principles of Fluorescence Spectroscopy*; Plenum Press: New York, 1983.

Table 4. Redox Properties of Photosensitizers[a]

photosensitizer	$E^{0'}$ $M^{n+}/M^{(n+1)+b}$ (V vs SCE)	ΔE_p (mV)	$E^{0'}$ L/L$^-$ (V vs SCE)	ΔE_p (mV)
$Ru(bpy)_3^{2+}$	+1.26	80	−1.36	75
$Ru(dmphen)_3^{2+}$	+1.11	60	−1.53	65
$Ir(ppy)_2(bpy)^+$	+1.25	65	−1.42	70
$Ir(ppy)_2(phen)^+$	+1.24	65	−1.42	80
$Ir(ppy)_2(dphphen)^+$	+1.23	75	−1.38	70
$Ir(F\text{-}mppy)_2(bpy)^+$	+1.38	75	−1.39	60
$Ir(F\text{-}mppy)_2(phen)^+$	+1.36	60	−1.39	80
$Ir(F\text{-}mppy)_2(dphphen)^+$	+1.36	75	−1.35	70

[a] Cyclic voltammetry was carried out at 100 mV/s in 0.1 M TBAH/CH_3CN at a Pt working electrode with a Pt counter electrode and Ag wire pseudo-reference. Ferrocene was used as an internal standard, and potentials are reported with respect to a saturated calomel (SCE) electrode. [b] For ruthenium complexes, $n = 2$; for iridium complexes, $n = 3$.

Table 5. Excited-State Redox Properties of Photosensitizers

photosensitizer	emission max (eV)	$E^{0'}$ $*M^{n+}/M^{(n+1)+a}$ (V vs SCE)	$E^{0'}$ $*M^{n+}/M^{(n-1)+a}$ (V vs SCE)
$Ru(bpy)_3^{2+}$	2.04	−0.78	+0.68
$Ru(dmphen)_3^{2+}$	2.07	−0.96	+0.54
$Ir(ppy)_2(bpy)^+$	2.10	−0.85	+0.68
$Ir(ppy)_2(phen)^+$	2.12	−0.88	+0.70
$Ir(ppy)_2(dphphen)^+$	2.08	−0.85	+0.70
$Ir(F\text{-}mppy)_2(bpy)^+$	2.20	−0.82	+0.81
$Ir(F\text{-}mppy)_2(phen)^+$	2.22	−0.86	+0.83
$Ir(F\text{-}mppy)_2(dphphen)^+$	2.20	−0.84	+0.85

[a] For ruthenium complexes, $n = 2$; for iridium complexes, $n = 3$.

observation (see Table 3) that the three F-mppy iridium compounds are more strongly quenched by TEOA (the sacrificial reductant which gets oxidized) than their ppy counterparts. It is plausible that the increased hydrogen production seen in the F-mppy compounds relative to the ppy compounds is due to the increased efficiency of a secondary pathway to hydrogen production via quenching of the excited photosensitizer by TEOA. However, from our work to date, a straightforward correlation between either quenching or electrochemical parameters and hydrogen production is not evident. This complexity lends credence to our decision to approach the investigation of this system with a parallel methodology.

Mechanistic Studies. The lack of clear correlations between the photophysical properties of our iridium photosensitizers and their performance in terms of hydrogen production led us to conduct several studies to try to elucidate information about the mechanism of the obviously complex catalytic process occurring. These studies were facilitated through the use of the high-throughput photophysical screening protocols described previously as well as by the multiwell apparatus and high-throughput hydrogen sensor described above.

One could easily envision a scenario in which hydrogen production is limited by the catalytic turnover of the photosensitizer molecule. Alternatively, hydrogen generation might instead be controlled by the catalytic limitations of the electron relay. The goal of our initial mechanistic study was to investigate the catalytic properties of the photosensitizer, specifically how many times the molecule could "turn over". For this investigation, we employed the "standard" sensitizer, $Ru(dmphen)_3^{2+}$, but ongoing research will extend this work to the iridium photosensitizers that have been discovered. The results shown in Table 2 indicate approximately the same number (ca. 800−900) of turnovers for most of the photosensitizers used, which

Table 6. Effect of Photosensitizer Concentration on Photoinduced Hydrogen Production[a]

photosensitizer concentration (μM)	H_2 evolved (μmol)	photosensitizer turnovers
0.50	43	9200
0.99	83	8900
2.5	160	6900
4.9	210	4500
7.4	300	4200
15	320	2300
17	390	2400
37	400	1100
74	377	540
296	383	140
320	401	130

[a] All samples have a total volume of 20 mL and contain the specified amount of $Ru(dmphen)_3^{2+}$ (the photosensitizer), 2.5 mM $Co(bpy)_3^{2+}$ (electron relay), 0.57 M TEOA, and 0.27 M LiCl in 50:50 water:acetonitrile. The pH was adjusted by the addition of 0.4 mL of 12 M HCl.

led us to question whether we were actually probing the performance limits of the photosensitizers. By decreasing the concentration of $Ru(dmphen)_3^{2+}$ used while keeping the concentration of electron relay constant, it was possible to establish an upper limit to the number of turnovers of the photosensitizer. The results from this experiment (the quantity of hydrogen evolved and the number of turnovers for the photosensitizer) can be seen in Table 6. Even at submicromolar photosensitizer concentrations, hydrogen was still produced. It appears that the $Ru(dmphen)_3^{2+}$ photosensitizer is capable of approximately 9000 turnovers. As will be discussed below, the photosensitizer appears not to be the limiting factor in the photoinduced production of hydrogen. In Figure 7, a plot of hydrogen production versus photosensitizer concentration can be seen.

When the photosensitizer concentration is low, the amount of hydrogen produced increases substantially with increasing photosensitizer concentration. However, as the concentration is increased, it appears that the amount of hydrogen produced reaches a plateau. We ascribe this behavior to the optical properties of the photosensitizer; if enough chromophore is present, all the light from the LED light sources will be absorbed and additional photosensitizer will have no effect. The amount of hydrogen evolved should be proportional to the amount of light energy collected and can be given by eq 5

$$H_2 = m(1 - 10^{-\epsilon L c}) \qquad (5)$$

where m is a proportionality constant, ϵ is the molar extinction coefficient of the chromophore, L is the path length of the system (approximately 3.5 cm from the bottom of the sample vial to the top of the solution), and c is the concentration of the photosensitizer. The solid line in Figure 7 is a fit of the data to eq 5, and it is clear that this model describes the data quite well, with an R^2 value of 0.9792.

To further probe this system, another set of experiments was carried out, varying the amount of $Co(bpy)_3^{2+}$ used while keeping a constant concentration of photosensitizer. For these experiments, a photosensitizer concentration was chosen that was in the "plateau region" described above. This choice was made to ensure that there was no variation in the amount of hydrogen produced due to the amount of photosensitizer present. The results of these experiments (the quantity of hydrogen evolved and the number of turnovers for the electron relay) are

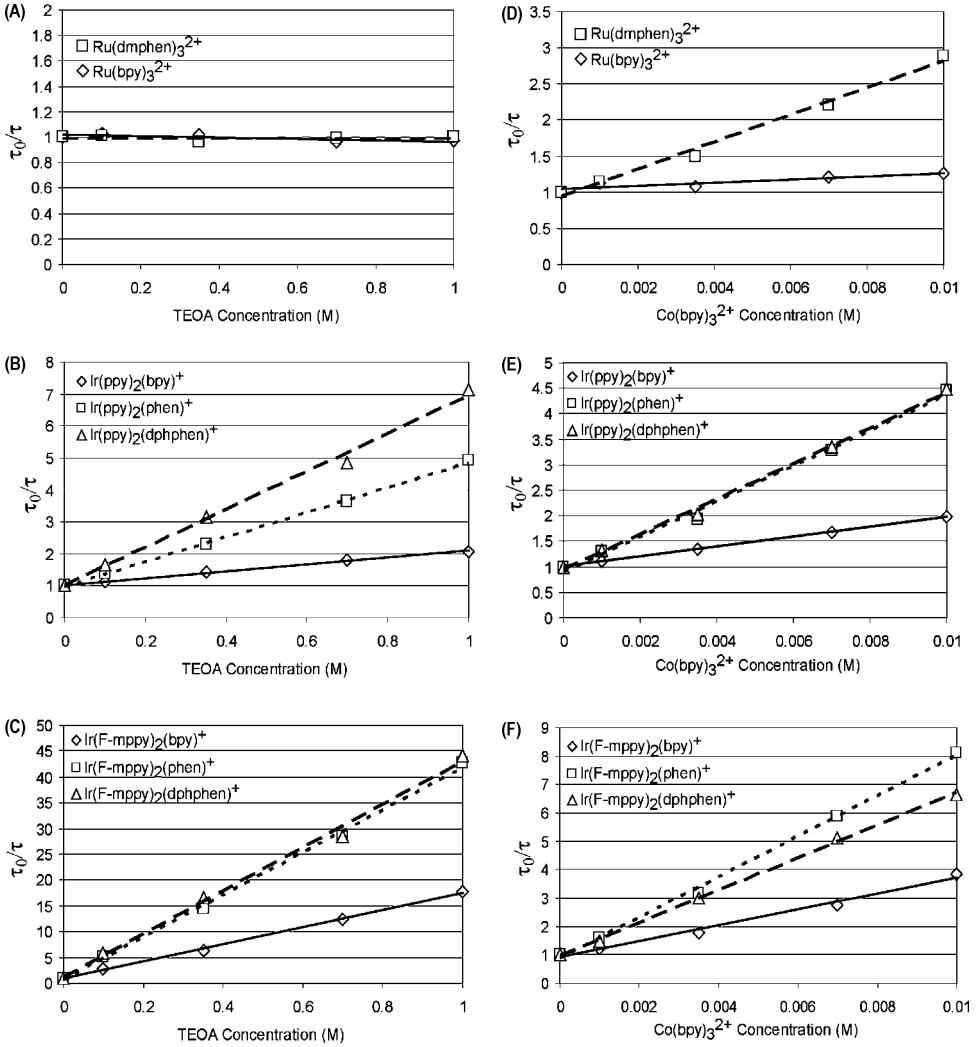

Figure 6. (A−C) Dynamic quenching studies of two ruthenium-based photosensitizers and six novel iridium photosensitizers by TEOA. (D−F) Dynamic quenching studies of two ruthenium-based photosensitizers and six novel iridium photosensitizers by $Co(bpy)_3^{2+}$. All linear fits shown have $R^2 > 0.99$.

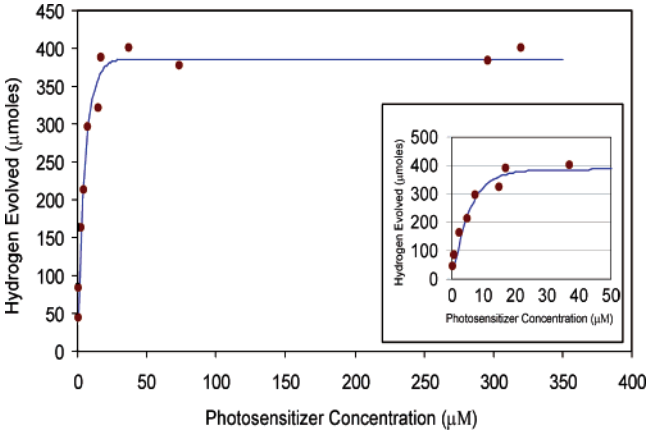

Figure 7. Hydrogen evolution versus concentration of $Ru(dmphen)_3^{2+}$ photosensitizer. In all cases, the concentration of electron relay $Co(bpy)_3^{2+}$ was 2.5 mM. The inset gives detail at low concentration. Solid line is a fit of data to eq 5 ($R^2 = 0.9792$).

Table 7. Effect of Electron Relay Concentration on Photoinduced Hydrogen Production[a]

$Co(bpy)_3^{2+}$ concentration (mM)	H_2 evolved (μmol)	$Co(bpy)_3^{2+}$ turnovers
0.17	120	74
0.46	140	31
0.88	210	24
1.25	220	18
1.83	300	16
2.50	270	11
5.0	360	7
10.0	332	3

[a] All samples have a total volume of 20 mL and contain 300 μM $Ru(dmphen)_3^{2+}$ (the photosensitizer), the specified amount of $Co(bpy)_3^{2+}$ (electron relay), 0.57 M TEOA, and 0.27 M LiCl in 50:50 water:acetonitrile. The pH was adjusted by the addition of 0.4 mL of 12 M HCl.

shown in Table 7. Additionally, a plot of hydrogen production versus electron relay concentration can be seen in Figure 8.

Superficially, the behavior shown in this plot appears similar to that for the photosensitizer; at low $Co(bpy)_3^{2+}$ concentrations, the amount of hydrogen produced increases, and at higher concentrations, it reaches a plateau. However, the function of the electron relay is to react with excited photosensitizer molecules, not to absorb light energy; hence, increasing the $Co(bpy)_3^{2+}$ concentration would not be expected to have the same effect as increasing the photosensitizer concentration. For the experiments described in Table 7, the concentration of the electron relay is changed by a factor of 60. However, the amount of hydrogen produced only changes by a factor of 3. At low

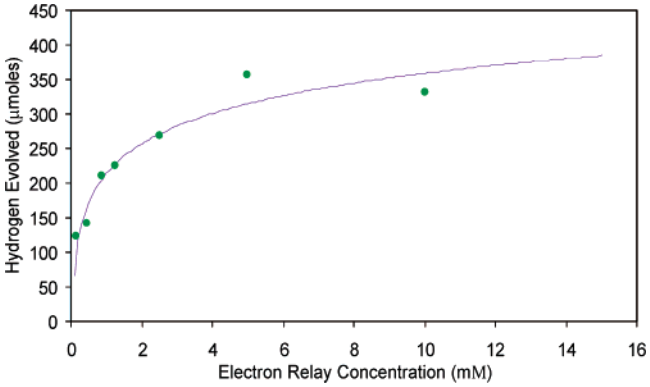

Figure 8. Hydrogen evolution versus concentration of $Co(bpy)_3^{2+}$ electron relay. In all cases, the concentration of the photosensitizer $Ru(dmphen)_3^{2+}$ was 300 μM. The solid line is a guide to the eye.

concentrations of $Co(bpy)_3^{2+}$, the electron relay is capable of more than 70 turnovers, while at very high concentrations, it only turns over several times. We postulate that this behavior is due to a reaction of the reduced (i.e., very reactive) electron relay molecules that yields an inactive cobalt species. The existence of this reaction would have the effect of destroying the electron relay and shutting off the production of hydrogen, and evidence of such a process will be detailed in a forthcoming manuscript.

Conclusions

In this work, we have demonstrated the combinatorial development of six heteroleptic iridium transition metal complexes that serve as extremely effective photosensitizers for the generation of hydrogen through the photocatalytic reduction of water. All six of these photosensitizers perform more efficiently than the current best photosensitizers. We have also shown that our methodology, which involves combinatorial synthesis, high-throughput photophysical screening, parallel photocatalytic reactions, and the use of a fast, selective hydrogen sensor, is an efficient and effective pathway for the advancement of science and technology in this area of research.

The ability to carry out photoinduced hydrogen generation experiments in parallel and to quickly analyze the gaseous products has enabled the acquisition of significant mechanistic understanding of the processes involved. While the photosensitizer is extremely catalytic (at least 9000 turnovers), the limiting factor in the generation of hydrogen appears to be the decay of the electron relay $Co(bpy)_3^{2+}$, which decomposes after less than 100 turnovers. Work is currently underway to optimize the electron relay through the application of the combinatorial, high-throughput methodology laid out in this paper.

Acknowledgment. We thank Nathan Speer and Robert Pendergrass at H2Scan for making the RobustHydrogenSensor available, as well as for useful discussions and generous technical support. We also thank Robert A. Pascal Jr. for the generous gift of laboratory equipment, and Andrew Bocarsly for the use of a potentiostat. S.B. acknowledges support from a Camille and Henry Dreyfus New Faculty Award and a NSF CAREER award (CHE-0449755). T.H.A. acknowledges support for summer research through Princeton University's Partners in Science Program.

Supporting Information Available: Procedures for the synthesis of the ligands F_2-mppy and Cl_2-mppy, as well as for the preparation of the six iridium complexes examined in this work. Structural identification via ^1H and ^{13}C NMR as well as by ESI−MS is also included. This material is available free of charge via the Internet at http://pubs.acs.org.

JA0427101